

# Strategies For Resolving Camera Metamers Using 3+1 Channel

Dilip K. Prasad  
Nanyang Technological University,  
School of Computer Science and Engineering, Singapore  
dilipprasad@gmail.com

## Abstract

This paper discusses the problem of reducing camera metamerism by using a fourth spectral channel in addition to the typical red, green, and blue channels of the tristimulus sensor used in the commercial consumer cameras. Specifically, we consider three options for this fourth channel. The first option is to use a color channel from another camera to reduce metamerism. The second option is to use a color channel from an image captured by the same camera but with a color filter as the fourth channel. The third option is to design a specific spectral channel to be fabricated with the existing camera sensor. This option uses the metameric black space to design the channel. The commercial cameras' original metamerism is typically more than 20%, as observed in a dataset of 335 spectral images captured in 5 different indoor illuminations. Our results show that the third option is the best since it reduces metamerism down to about 5%. Among the first and second options, the first option is more effective and it reduces metamerism down to about 15%. The channel designed using the third option can be used for advanced applications such as distinguishing objects with different spectral reflectances but similar colors.

## 1. Introduction

Metamerism is the term given to the phenomenon where different spectral power distributions in a scene map to the same apparent color under a tristimulus imaging system, such as the human visual system or an RGB camera [23]. Two or more objects that have the same tristimulus response in an imaging system are called metamers. Fig. 1 gives an example of this problem, where an orange and a carrot have the same apparent color (i.e. same RGB values) even though their spectral reflectances are notably different. For the human visual system, metamerism is not an undesirable phenomenon as it allows us to reproduce the apparent colors of objects using inks and dyes and even creating optical illusions [24]. However, for color reproduction

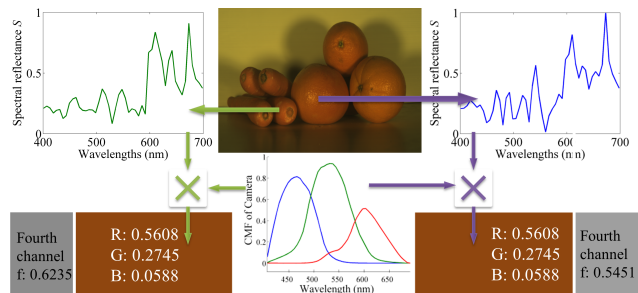


Figure 1. Two objects with different spectral reflectances that have the same RGB color values are shown here. These are known as metamers. We propose to use a fourth color channel to resolve or distinguish the metamers.

across various sensors [22] and other computer vision tasks [16, 20], sensor metamerism is undesirable.

Camera sensors use spectral filters (one for each red, green, and blue color channel) to obtain a tristimulus response for color reproduction. These filters are often referred to as the color matching functions (CMF) of the camera. Owing to the projective nature of imaging, the original spectral input gets projected to only three color values through the CMF. Due to the projection of a large-dimensional spectral input to only 3-dimensional color data (i.e., the channel responses), sensor metamerism is unavoidable. However, if the dimensionality (i.e., number of channels) of the camera data can be increased, for example using additional channels or by using non traditional cameras [4, 6, 31, 36, 39, 28], then the amount of metamerism can be reduced. This is the central idea of this paper. We note that some works use near infrared as an additional channel [14, 32, 33]. But, this work focuses on using visible range solutions only.

To this end, we consider several options to increase the dimensionality of the camera using an extra channel, as shown in Fig. 2. One option is to linearly combine one of the RGB channel responses from another camera with the respective channel response of the camera whose metamerism is to be reduced (called the target camera for simplicity) and use it as the fourth channel response. The second option is to capture the same scene using the same

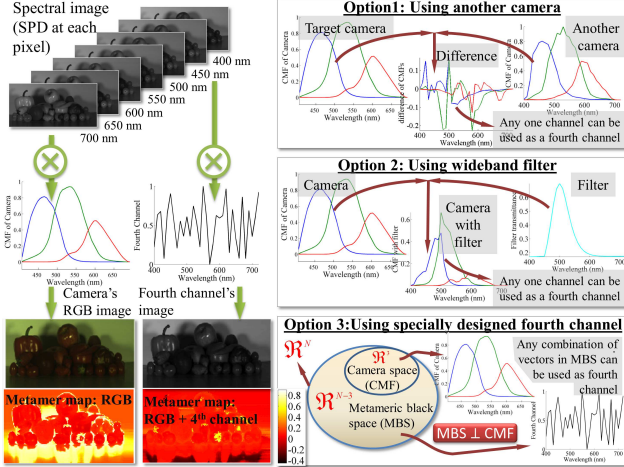


Figure 2. Metamerism can be reduced using a fourth channel as illustrated on the left side. The three options, namely, using a channel from another camera, using a filter, and using a specifically designed channel, are illustrated on the right side.

camera but through a wideband filter and then use one of the channel responses from the filtered image as the fourth channel response. These two options use existing camera sensor or filter. The third option is to design an additional color channel that is orthogonal to the CMF of the target camera and fabricate it with the target camera's color filter array.

In addition to considering the various options, we also propose a measure in eq. (6) to theoretically evaluate the suitability of the various options. Also, we present a simple pixel-wise method to calculate the statistics of metamerism in an image using the metrics in eq. (7). Our results show that the specifically designed filter, i.e., the third option, gives the best performance among the three options. We consider five commercial cameras: Canon 1D Mark III, Canon 600D, Nikon D40, Nikon D5100, and Sony  $\alpha 7$ . Their CMF are given in the *supplementary material*. We also show in section 7 how the fourth channel can be used to distinguish objects with similar color but different spectral properties using a simple clustering approach. Examples include distinguishing carrots and oranges (see Fig. 1) and real and fake apples.

In the remainder of the paper, section 2 discusses related work on the problem of metamerism while section 3 presents technical background of metamerism and section 4 presents the quantitative metric to measure metamerism. Section 5 presents the details of the three options for reducing metamerism and section 6 presents numerical results of metamerism reduction using the different options. Section 7 shows how the fourth channel can help in differentiating between two similarly colored objects. Section 8 concludes the paper. The *supplementary material* presents additional details such as the illumination spectra, the CMFs, and the result of distinguishing objects for

different cameras.

## 2. Related work

Metamerism was statistically studied in [3, 5, 13, 25]. Ref. [3, 13, 25] studied the crossover wavelengths of a wide range of incoming metameric spectral power distributions (SPDs) on a sensor. Ref. [5] statistically derived the spatio-spectral bases to represent hyperspectral images and suggested that using another channel in addition to the CMF may be useful in reducing metamerism. Analyses of spectral reflectances of standard color charts/chips and natural objects [7, 12, 19, 26] have also indicated statistically that three channels, such as in tristimulus devices, are not sufficient for representing the spectral content of a scene very well and the adequate dimensionality of the spectral information is larger than three. The general conclusion of [5, 7, 12, 18, 19, 26] is that 4 to 10 known bases (equivalent to 4 to 10 color channels) are needed for retaining sufficient spectral information. Thus, researchers have considered the use of more than three color channels. For example, [36] used seven color channels for controlling dynamic range, spectral sensitivity, and other aspects of image capturing. Six channels system [17] and four channels system [21] were investigated for extending the color gamuts of camera. Six channels color printer was proposed in [34] for reducing metamerism in printing. Two overlapping but shiftable CMY color filter arrays were used to obtain both CMY color channels and RGB color channels in [31].

The issue of metamerism and the concept of metameric blacks is known for several decades [35]. Cohen and Kappauf developed this concept further by proposing a matrix-R theory that uses an orthogonal projector, termed  $\mathbf{R}$  (thus the name matrix-R), to decompose an incoming SPD into two components mathematically [8]. Accordingly [8], the incoming SPD from any point in a scene can be split into two components: a *fundamental metamer* and a *metameric black* vector. The fundamental metamer is unique to the channel responses. It is a definite linear combination of the CMF and responsible for the observed tristimulus response. The metameric black vector projects to  $[0, 0, 0]$  in the color space and lies completely in the space orthogonal to the CMF, thus does not contribute to the tristimulus response. The space orthogonal to the CMF is known as the metameric black space (MBS). Two metameric objects can be modeled as having the same fundamental metamer, but different metameric black vectors.

In some situations, metamerism and MBS can be exploited. For example, [9] used metamerism for the application of watermarking [2]. In [9], the problem of separating metamers of a display device using an optimized  $3 \times 3$  matrix transform on a camera was addressed so that metamers that visually look similar in the display

device can be distinguished using the optimized matrix and the camera. In [1, 37], metameric blacks were used for calibrating cameras by determining their CMF. The idea was to subtract the mean spectral reflectance from a set of known metameric spectral reflectances, which would give an estimate of MBS. Once MBS was known, CMF was computed as the vectors orthogonal to this space and resulting in the reference tristimulus response. Another example is the problem of reconstructing spectral reflectances of objects in a scene using MBS [10, 11, 27, 38]. Once the fundamental metamer of an object was known through its tristimulus response and the camera's CMF, the problem of reconstructing the reflectance required estimation of the linear combinations of the bases of the MBS.

In this paper, we use MBS to assess the suitability of the chosen channel for reducing metamerism. Further, we use MBS to design a fourth channel that specifically images the metameric black vector of an incoming SPD.

### 3. Metameric black space

Here, we introduce the concept of metameric black space. Let the camera's CMF be denoted as:

$$\mathbf{C} = \begin{bmatrix} \bar{R}^T \\ \bar{G}^T \\ \bar{B}^T \end{bmatrix} = \begin{bmatrix} R(\lambda_1) & R(\lambda_2) & \cdots & R(\lambda_N) \\ G(\lambda_1) & G(\lambda_2) & \cdots & G(\lambda_N) \\ B(\lambda_1) & B(\lambda_2) & \cdots & B(\lambda_N) \end{bmatrix}, \quad (1)$$

where  $\lambda_n$  indicates the  $n^{\text{th}}$  wavelength, and  $R(\lambda), G(\lambda), B(\lambda)$  represent the red, green, and blue channels' spectral sensitivities. Consider an incoming SPD from a scene  $\bar{S} = [S(\lambda_1) \ S(\lambda_2) \ \cdots \ S(\lambda_N)]^T$ . Physically, the SPD  $\bar{S}$  is the element-wise product of the illumination spectrum and the spectral reflectance of a point in the scene. In the Lambertian model of image formation [15], the color value  $\bar{X} = [r \ g \ b]^T$  corresponding to this SPD is given as:

$$\bar{X} = \mathbf{C}\bar{S}. \quad (2)$$

According to the matrix-R theory [8], an SPD can be decomposed into two parts - one is a fundamental metamer which is a linear combination of the CMFs and the other is a combination of the metameric blacks which are vectors orthogonal to the CMFs. The matrix-R theory defines an operator  $\mathbf{R}$  as follows:

$$\mathbf{R} = \mathbf{C}^T (\mathbf{C}\mathbf{C}^T)^{-1} \mathbf{C}. \quad (3)$$

The fundamental metamer  $\bar{S}_0$  of the SPD  $\bar{S}$  is given by  $\bar{S}_0 = \mathbf{R}\bar{S}$ . and the metameric black  $\bar{S}_b$  of  $\bar{S}$  is given by:

$$\bar{S}_b = (\mathbf{I} - \mathbf{R})\bar{S}, \quad (4)$$

where  $\mathbf{I}$  is the identity matrix. Further,  $\bar{S}_b$  satisfies the equation below:

$$\mathbf{C}\bar{S}_b = \mathbf{C}(\mathbf{I} - \mathbf{R})\bar{S} = [0, 0, 0]^T, \quad (5)$$

which shows that CMFs are orthogonal to the metameric black  $\bar{S}_b$ . The mathematical range of  $(\mathbf{I} - \mathbf{R})$  forms the space of the metameric blacks. This space is thus spanned by the left singular vectors corresponding to the non-zero singular values of  $(\mathbf{I} - \mathbf{R})$ . Since the CMF of a tristimulus device has three independent channels, it is easy to see that the number of non-zero singular values is  $(N - 3)$ . Let the left singular vectors corresponding to the non-zero singular values be represented as  $\bar{u}_n, n = 1$  to  $(N - 3)$  and corresponding to the zero singular values be represented as  $\bar{u}'_{n'}, n' = 1$  to 3. Then, the MBS is spanned by the vectors in a set  $\underline{\mathbf{M}} : \{\bar{u}_n\}$  and CMF is spanned by the vectors in a set  $\underline{\mathbf{C}} : \{\bar{u}'_{n'}\}$ .

It is interesting to note that any spectral vector in the MBS does not contribute to the RGB color at all due to the orthogonality between the MBS and the CMF. This fact gives an important insight that the MBS is a property of the camera's CMF only and has no relation at all to the color point. As a consequence, the fourth channel needs to target the MBS only and need not cater to every color value individually. An ideal fourth channel for reducing metamerism should be orthogonal to the CMF and should be given as a linear combination of  $\{\bar{u}_n, n = 1$  to  $(N - 3)\}$  only. So, the theoretical suitability of the fourth color channel  $\bar{F} = [F(\lambda_1) \ F(\lambda_2) \ \cdots \ F(\lambda_N)]^T$  can be assessed using the following metric:

$$\alpha(\bar{F}) = \sqrt{\frac{\sum_{n'=1}^3 (\bar{u}'_{n'}^T \bar{F})^2}{\sum_{n=1}^{N-3} (\bar{u}_n^T \bar{F})^2}}. \quad (6)$$

This metric  $\alpha$  is the ratio of the projection of the channel  $\bar{F}$  onto the CMF to the projection of the channel  $\bar{F}$  onto the MBS. The smaller the value of  $\alpha(\bar{F})$ , the more suitable is the channel for resolving metamers and reducing metamerism, since it contains larger information from MBS.

### 4. Measuring metamerism in an image

Let us consider two incoming SPDs  $\vec{S}_1$  and  $\vec{S}_2$ , and the color values corresponding to them  $\vec{X}_1 = \mathbf{C}^T \vec{S}_1$  and  $\vec{X}_2 = \mathbf{C}^T \vec{S}_2$ . The angular difference (AD) between these two SPDs in the spectral domain and the camera's color space are quantified as:

$$\theta_\Omega = \angle(\vec{S}_1, \vec{S}_2); \quad \theta_{\text{RGB}} = \angle(\vec{X}_1, \vec{X}_2). \quad (7)$$

If  $\theta_\Omega > \theta_0$ , where  $\theta_0$  is an appropriately chosen threshold, then  $\vec{S}_1$  and  $\vec{S}_2$  are dissimilar in the spectral sense. Similarly, if  $\theta_{\text{RGB}} > \theta_0$ , then they are dissimilar in the camera's color space. Metamerism occurs if  $\theta_\Omega > \theta_0 > \theta_{\text{RGB}}$ .

For a pixel  $p$  in a given image with total number of pixels  $P$ , we find the percentage of pixels  $U(p)$  that are spectrally

dissimilar to the SPD  $\bar{S}_p$  of the pixel  $p$ . Similarly, we find the percentage of pixels  $V(p)$  whose color values are dissimilar to the color value  $\bar{X}_p$  of the pixel  $p$ . Then the percentage of metamers at pixel  $p$  are given by  $M(p) = U(p) - V(p)$ .

We note that two pixels may be similar if they belong to the same object under similar conditions, or if they are metameric. However, dissimilar pixels are definitely non-metameric. Thus,  $U(p)$  and  $V(p)$  can be written as:

$$U(p) = 1 - (U_{\text{sim}} + U_{\text{met}}), \quad (8)$$

$$V(p) = 1 - (V_{\text{sim}} + V_{\text{met}}), \quad (9)$$

where  $U_{\text{sim}}$  and  $V_{\text{sim}}$  are the percentage of pixels belonging to similar objects as the pixel  $p$ , as measurable in the spectral domain and camera's color space respectively. Ideally,  $U_{\text{sim}} = V_{\text{sim}}$ .  $U_{\text{met}}$  and  $V_{\text{met}}$  are the percentage of pixels metameric to the pixel  $p$  in the spectral domain and camera's color space, respectively. Using (8) and (9),  $M(p) \approx V_{\text{met}}(p) - U_{\text{met}}(p)$ , if  $U_{\text{sim}} \approx V_{\text{sim}}$ , a condition which can be ensured by choosing a suitable value of threshold  $\theta_0$ .

In a strict sense, a suitable value of  $\theta_0$  should be chosen on a case-by-case basis. Having said that, we are not aware of an adaptive method suitable for our case which allows us to choose thresholds for different images and objects. Thus, we have resorted to the use of constant threshold value  $\theta_0 = 8^\circ$ , which corresponds to  $\cos(\theta_0) = 0.9903$ , indicating that two functions are considered dissimilar if their projection on each other is more than 0.9903.

An illustration of  $U(p)$ ,  $V(p)$  and the metamer map  $M(p)$  is shown in Fig. 3 for the example image in Fig. 2. In Fig. 3(a,b), which show  $U(p)$  and  $V(p)$  respectively, a higher value indicates higher dissimilarity in the spectral space or the camera's color space, respectively. In Fig. 3(c), which shows  $M(p)$ , values close to zero indicate smaller amount of metamerism in the camera's color space.

We note that strict digital equivalence of the tristimulus responses can also be used as an explicit measure of metamerism. But, it is sensitive to sensor noise while the above approach is not sensitive to sensor noise.

## 5. Options for fourth channel

In this section, we present the different options for forming a fourth color channel and discuss their suitability for the problem of reducing metamerism. The three options are discussed next.

### 5.1. Option 1: Using one channel response from another camera

Suppose the CMF of the target camera, in the form of eq. (1), is given by  $\mathbf{C}_1$  and the tristimulus response of this camera to an incoming SPD is denoted as

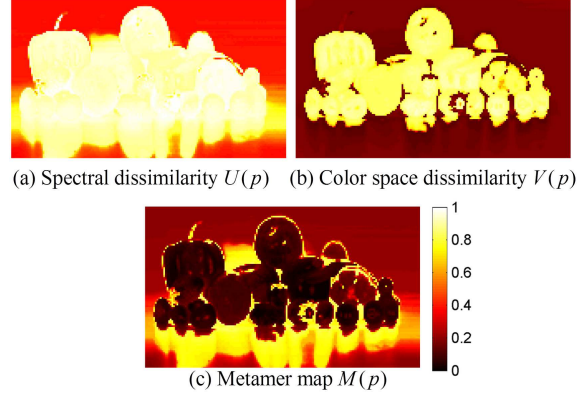


Figure 3. Illustration of measurement of the amount of metamerism in an image is given here.

$\bar{X}_1 = [r_1 \ g_1 \ b_1]^T$ . Also, suppose that  $\bar{X}_2 = [r_2 \ g_2 \ b_2]^T$  is the tristimulus response of another camera with CMF  $\mathbf{C}_2$  to the same SPD. Then, we can form a hypothetical tristimulus response  $\bar{X}' = [r' \ g' \ b']^T = \bar{X}_1 - \bar{X}_2$  created due to a hypothetical CMF  $\mathbf{C}' = \mathbf{C}_1 - \mathbf{C}_2 = [\bar{R}' \ \bar{G}' \ \bar{B}']^T$ .

We can choose either  $\bar{R}'$ , or  $\bar{G}'$ , or  $\bar{B}'$  as the fourth color channel and the corresponding  $r'$ ,  $g'$ , or  $b'$  as the channel response  $f$  of the fourth channel and form a new color value  $\bar{Y} = [r_1 \ g_1 \ b_1 \ f]^T$ . In principle, all the three channels  $\bar{R}'$ ,  $\bar{G}'$ ,  $\bar{B}'$  can be used as additional channels. But, we restrict ourselves to the use of only one extra channel. We also note that using all the three additional channels improves the results only marginally over the results obtained using the best channel. The choice of the best channel is discussed later in section 5.4. An example of  $\mathbf{C}'$  formed for target camera Canon 1D Mark III and the other camera Nikon D5100 is shown in Fig. 4(a).

### 5.2. Option 2: Using a filter

Suppose that a scene is captured using a camera with the CMF  $\mathbf{C}$  directly as well as through a filter with filter response (transmittance)  $\bar{K} = [K(\lambda_1) \ K(\lambda_2) \ \dots \ K(\lambda_N)]^T$ . Then the CMF of the camera with the attached filter is given by  $\mathbf{C}' = \text{diag}(\bar{K})\mathbf{C} = [\bar{R}' \ \bar{G}' \ \bar{B}']^T$  and its tristimulus response is given by  $\bar{X}' = [r' \ g' \ b']^T = \mathbf{C}'\bar{S}$ . As in section 5.1, we can choose either  $\bar{R}'$ , or  $\bar{G}'$ , or  $\bar{B}'$  as the fourth color channel and the corresponding  $r'$ ,  $g'$ , or  $b'$  as its tristimulus response  $f$ , resulting in the new color value  $\bar{Y} = [r_1 \ g_1 \ b_1 \ f]^T$ . An example of  $\mathbf{C}'$  formed for target camera Canon 1D Mark III and a cyan filter is shown in Fig. 4(b).

We have considered two filters (cyan and yellow) shown in Fig. 5, which correspond to Andover company's filters with part numbers 500FS80-25 and 600FS80-25,

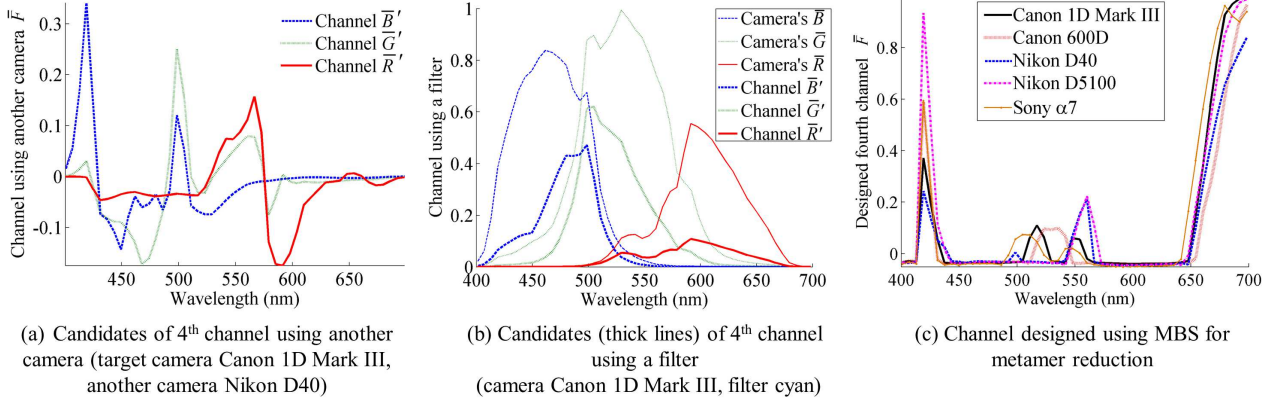


Figure 4. Examples of candidate channels for the fourth channel for reducing metamerism are shown here.

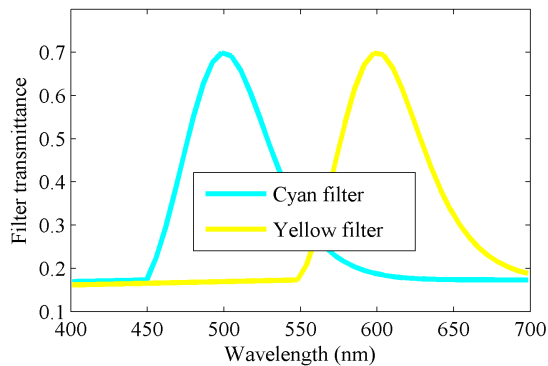


Figure 5. Cyan and yellow filters considered for reducing metamerism.

respectively. We choose these filters since they roughly cover one of the nulls between the three channels.

### 5.3. Option 3: Specific channel design using MBS

Now, we consider the design of a channel for the specific purpose of reducing metamerism. Since the fourth channel should target the MBS only, the spectral sensitivity  $\bar{F}$  of the fourth channel should be a linear combination of the vectors in  $\underline{\mathbf{M}}$ :

$$\bar{F} = \sum_{n=1}^{N-3} a_n \bar{u}_n \quad (10)$$

For achieving a practical channel,  $\bar{F}$  should be positive valued. Thus, the solution of  $\{a_n\}$  is obtained as  $\arg \min_{\{a_n\}} \left( \sum_{\forall n} (|F(\lambda_n)| - F(\lambda_n))^k \right)$ , where  $k$  determines the severity of optimization. In our observation, small values of  $k$  suppress several frequency components while large values of  $k$  are not effective in making  $\bar{F}$  positive valued. Also, our observation is that  $k = 9$  generally gives good solution with about three frequency bands and small negative floor value, as seen for the five cameras in Fig. 4(c). We denote the designed filter as  $\bar{F}'$ . Channel that

can be practically fabricated is obtained by truncating the negative values of  $\bar{F}$  to zero. We denote this fabricable practical filter as  $\bar{F}'$ . We note that the complete spectral data was measured using hyperspectral camera and then the fourth channel's data is generated computationally by applying the filter.

### 5.4. Suitability for metamer reduction

In order to assess the suitability of these various options, for each option, we compute  $\alpha$  using eq. (6). Table 1 lists the values of  $\alpha$  of the various options for the five commercial cameras considered in this paper. It is seen that the option of using filters is not quite suitable since the values of  $\alpha$  are typically more than 1 for all channels and all cameras. If at all, the cyan filter's blue channel is the most suited among other channels. The option of using another camera fares better with the value of  $\alpha$  being less than 1 for most camera and channel combinations. We note that pairing Canon 1D Mark III and Nikon D5100 and using their blue channel's difference as the fourth channels suits both of them better than the other combinations. Similarly, the blue channel's difference for Nikon D40 and Sony  $\alpha$ 7 cameras suit both of them better. In fact using Nikon D40's blue channel for reducing metamers of Sony  $\alpha$ 7 camera should be especially effective as shown by a very small value of  $\alpha = 0.08$ . Thus, in general, blue channel appears to be more suitable for metamer reduction using another camera. Canon 600D is however an exception, for which Canon 1D Mark III camera's red channel is the best suited. Finally, the specific channel designed using MBS  $\bar{F}$  is the best suited since the values of  $\alpha$  for all the cameras are of the order of  $10^{-16}$  or lower. Even its practical version  $\bar{F}'$  obtained by truncating negative values to zero still performs better than the other options (using another camera or filter), except for Sony  $\alpha$ 7 camera, where they are comparable.

Based on the above study, for the remainder of the paper, we use the best combination of another camera and channel for each camera as the choice for the first option, cyan

Table 1. Table listing the values of  $\alpha$  for various options and different cameras.

	Canon 1D Mark III	Canon 600D	Nikon D40	Nikon D5100	Sony $\alpha 7$
Option 1, Canon 1D Mark III as another camera					
$\bar{R}'$	–	<b>0.43</b>	0.47	1.16	2.41
$\bar{G}'$	–	0.91	0.47	0.79	0.55
$\bar{B}'$	–	0.67	0.43	<b>0.43</b>	0.55
Option 1, Canon 600D as another camera					
$\bar{R}'$	0.38	–	0.58	1.01	2.55
$\bar{G}'$	0.86	–	0.99	0.81	0.96
$\bar{B}'$	0.76	–	0.77	0.98	1.45
Option 1, Nikon D40 as another camera					
$\bar{R}'$	0.36	0.47	–	2.13	3.78
$\bar{G}'$	0.56	1.11	–	1.60	0.92
$\bar{B}'$	0.45	0.67	–	0.50	<b>0.08</b>
Option 1, Nikon D5100 as another camera					
$\bar{R}'$	0.82	0.66	1.61	–	3.68
$\bar{G}'$	0.78	0.97	1.02	–	1.26
$\bar{B}'$	<b>0.26</b>	0.78	0.44	–	1.08
Option 1, Sony $\alpha 7$ as another camera					
$\bar{R}'$	4.61	4.82	7.30	8.30	–
$\bar{G}'$	0.76	1.10	0.99	1.51	–
$\bar{B}'$	0.80	1.79	<b>0.25</b>	1.29	–
Option 2, Cyan filter					
$\bar{R}'$	11.41	28.90	10.03	8.87	11.99
$\bar{G}'$	3.29	3.35	3.11	3.14	3.24
$\bar{B}'$	<b>2.14</b>	<b>2.31</b>	<b>1.95</b>	<b>2.13</b>	<b>1.98</b>
Option 2, Yellow filter					
$\bar{R}'$	4.88	4.48	6.23	5.92	6.50
$\bar{G}'$	3.16	3.15	3.04	3.17	3.22
$\bar{B}'$	105.38	31.52	97.03	76.24	75.55
Option 3: Specific design filter					
$\bar{F}$	0.00	0.00	0.00	0.00	0.00
$\bar{F}'$	0.08	0.11	0.11	0.08	0.08



Figure 6. Sample images from the dataset of spectral images [29] mapped to CIE XYZ color values are shown here.

filter’s blue channel as the choice for the second option, and specific channel  $\bar{F}$  and its practical version  $\bar{F}'$  as the third option.

## 6. Numerical results on a spectral dataset

This section presents numerical results of metamer reduction using the different options of fourth channel on a dataset of spectral images [29].

**Dataset of spectral images** The dataset contains 335 spectral images of fruits and vegetables taken using Specim’s PFD-CL-65-V10E (400 nm to 1000 nm) spectral camera. We have used OLE23 fore lens (400 nm to 1000 nm), also from Specim. Images in the dataset are captured under 5 different indoor illuminations of wide band metal halide lights (color temperatures - 2500 K, 3000 K, 3500 K, 4300K, and 6500K). The illumination spectra of these lights are given in the *supplementary material*. Since a scene is imaged under 5 illuminations separately, there are a total of 67 scenes. For each spectral image, a total of 49 bands were used for imaging (400 nm to 700 nm). Sample images from our dataset mapped to the CIE XYZ colorspace are shown in Fig. 6. About half of the scenes contain 24 patch ColorChecker Classic color chart in them.

**Statistical metric and example of metamer reduction** Let the RGB metamer map of an image, computed using the metric in section 4, be denoted as  $M(p)$ , briefly denoted as  $M$ . Let the color value using the fourth channel be denoted as  $\bar{Y} = [r \ g \ b \ f]^T$ , where  $f$  is normalized by the maximum value of the fourth channel’s responses for all the pixels in an image. This normalization is done for increasing the contrast in the fourth channel. Then, following section 4 and eq. (7), the angular difference between two RGBF color values  $\bar{Y}_1$  and  $\bar{Y}_2$  corresponding to two incoming SPDs  $\bar{S}_1$  and  $\bar{S}_2$  is given as:

$$\theta_{\text{RGBF}} = \angle(\bar{Y}_1, \bar{Y}_2) \quad (11)$$

The percentage of pixels in an image that are dissimilar to a pixel  $p$ , i.e.  $\theta_{\text{RGBF}} > \theta_0$ , be denoted as  $V'(p)$ . Then the RGBF metamer map with the fourth channel is  $M'(p) = U(p) - V'(p)$ , briefly denoted as  $M'$ . We can also compute the pixelwise reduction in metamerism as  $\delta M(p) = M(p) - M'(p)$ .

Considering the image shown in Fig. 2 as an example, we show the metamer reduction maps obtained using the different options of fourth channels in Fig. 7. Fig. 7(a,b) show the original image and its metamer map  $M$  for Canon 1D Mark III camera. The result for the fourth channel using Nikon D5100’s  $\bar{B}'$  channel (best option among other cameras as seen in Table 1) is shown in Fig. 7(c,d) using the metamer reduction map  $\delta M = M - M'$  and RGBF metamer map  $M'$ , respectively. Similarly, results for cyan filter’s  $\bar{B}'$  channel, specific design  $\bar{F}$ , and practical design  $\bar{F}'$  are shown in Fig. 7(e,f), Fig. 7(g,h), and Fig. 7(i,j), respectively. It is seen that the specific filter  $\bar{F}$  is the best in reducing metamerism, followed by the practical design  $\bar{F}'$ ,

Table 2. Table listing the statistics of reduction in metamerism using different options for different cameras.

Option	Metamerism mean( $M$ ) or mean( $M'$ )	Reduction mean( $\delta M$ )
	Units %	Units %
Canon 1D Mark III		
Original	24.34	—
Nikon D5100, $\bar{B}'$	17.01	7.33
Cyan Filter, $\bar{B}'$	22.42	1.92
Specific design $\bar{F}$	<b>7.22</b>	<b>17.12</b>
Practical channel $\bar{F}'$	11.22	13.12
Canon 600D		
Original	22.61	—
Canon 1D Mark III, $\bar{R}'$	19.58	3.03
Cyan Filter, $\bar{B}'$	21.95	0.66
Specific design $\bar{F}$	<b>4.32</b>	<b>18.29</b>
Practical channel $\bar{F}'$	8.96	13.65
Nikon D40		
Original	23.53	—
Sony $\alpha 7$ , $\bar{B}'$	18.35	5.18
Cyan Filter, $\bar{B}'$	21.07	2.46
Specific design $\bar{F}$	<b>6.17</b>	<b>17.31</b>
Practical channel $\bar{F}'$	9.92	13.61
Nikon D5100		
Original	23.97	—
Canon 1D Mark III, $\bar{B}'$	18.43	5.54
Cyan Filter, $\bar{B}'$	22.04	1.93
Specific design $\bar{F}$	<b>5.99</b>	<b>17.98</b>
Practical channel $\bar{F}'$	11.43	12.54
Sony $\alpha 7$		
Original	24.32	—
Nikon D40, $\bar{B}'$	12.13	12.19
Cyan Filter, $\bar{B}'$	23.55	0.77
Specific design $\bar{F}$	<b>7.25</b>	<b>17.07</b>
Practical channel $\bar{F}'$	11.29	13.03

Nikon D5100's  $\bar{B}'$  channel, and the cyan filter's  $\bar{B}'$  channel, in that order. This agrees well with observations in Table 1.

**Results on the entire dataset** In order to generate dataset level statistics, we compute the mean of  $M, M'$ , and  $\delta M$  for all the pixels in the dataset. The statistics for all the images in our dataset and for the 5 cameras is given in Table 2. It is seen that the specific design of the fourth channel performs the best, reducing the metamerism to a small percentage for all the cameras. Even the practical filter is able to reduce metamerism by about 13 % for all the cameras. On the other hand, the option of using filter is ineffective since it reduces metamerism by a very small percentage.

## 7. Example application: discriminating objects

Here, we consider an application of classifying two objects with similar colors but different spectral properties. Many objects, such as oranges and carrots have similar colors in most illuminations and most cameras. Thus, a vision application needs to rely on depth and shape for discriminating them. Even this approach fails when the

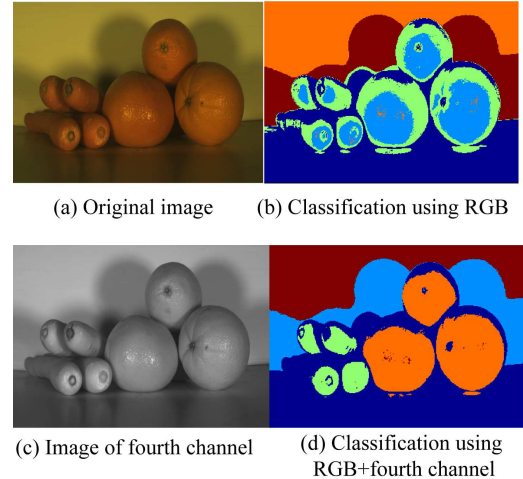


Figure 8. Example of discriminating between carrots and oranges using fourth color channel is shown here. Their SPDs are shown in Fig. 1.

objects have similar shapes and depths, such as in an image of real and fake apples. We show that distinguishability of such objects can be improved using the specific design of the fourth channel.

**Example 1: carrots and oranges** We consider an image of oranges and carrots shown in Fig. 8(a). A k-means clustering with 5 classes,  $k = 5$ , using only the RGB image gives the classification result shown in Fig. 8(b). However, k-means clustering with  $k = 5$  using RGB and fourth channel response  $f$  (Fig. 8(c)) results in clustering result shown in Fig. 8(d). It is seen that certain patches on carrots are distinguished from patches on oranges.

**Example 2: real and fake apples** We consider an image containing real and fake apples (see Fig. 9(a)). A k-means clustering on RGB image with 10 classes gives classification results as shown in Fig. 9(b) and the fake apple is not necessarily distinguished from the real ones. This is because all the classes assigned to the fake apple are assigned to at least one real apple too. On the other hand, the image of fourth channel in Fig. 9(c) shows a clear contrast of the fake apple with the real apples and the k-means clustering results shown in Fig. 9(d) indicates that at least two classes assigned to the fake apple were not assigned to any of the real apples. Thus, the fake apple is clearly distinguished from the real apples.

## 8. Summary and conclusion

The problem of metamerism in tristimulus devices such as consumer cameras is addressed in this paper. The root cause of metamerism is that the 3-dimensional information captured by the CMF of the camera is significantly less dimensional than the dimensionality of the spaces of incoming SPDs. Thus, the problem can be alleviated by using an additional channel that increases the

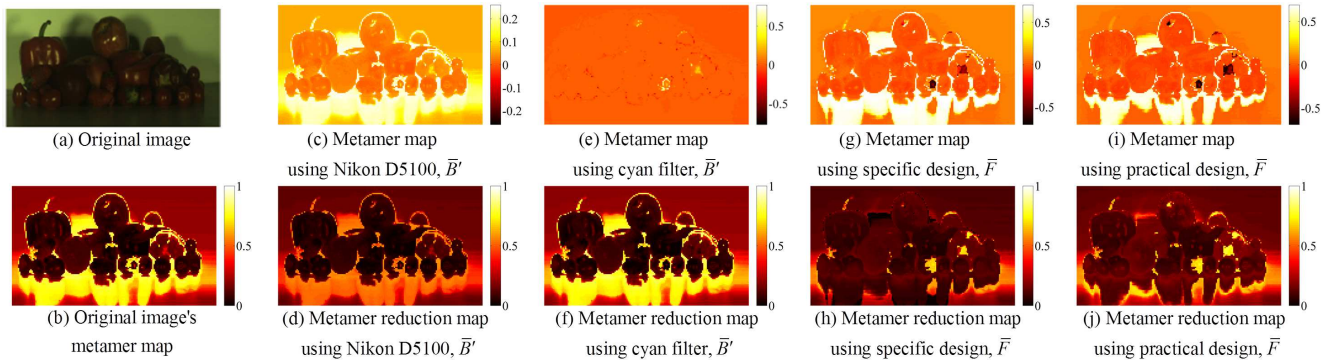


Figure 7. Example of reduction of metamerism using different options (note that the color bars in the top row are of different scale for the ease of visualization).

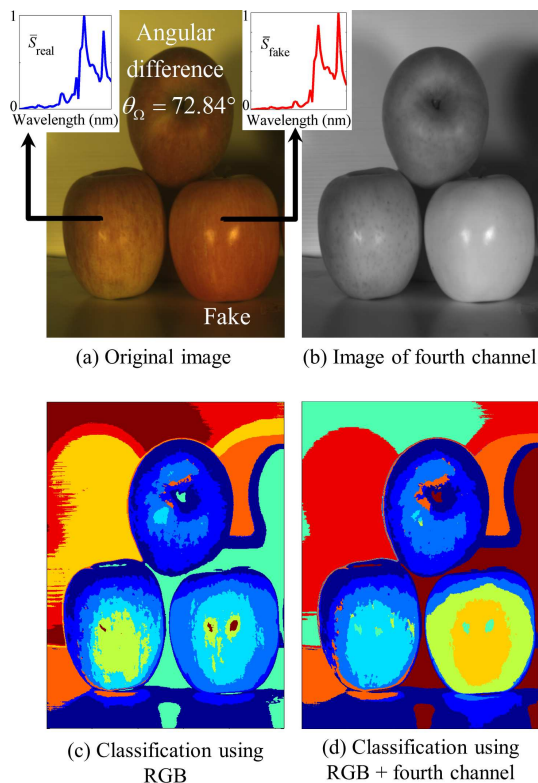


Figure 9. Example of discriminating between real and fake apples using fourth color channel is shown here. Their spectral reflectances are shown in the insets in subfigure (a). It is notable that the angular difference between the SPDs of real and fake apples is quite large,  $\theta_{\Omega} = 72.84^{\circ}$ , though they appear to have similar colors.

dimensionality of the data and has a small projection on CMF.

Three options for the fourth channel are discussed, viz. using a channel from another camera, using a color filter, and using an additional spectral channel in the sensor. The additional spectral channel is designed from the MBS of the camera. While the first two do not require changes in fabrication, they are not so effective in reducing

metamerism. On the other hand, the third option is very effective in reducing metamerism.

This is shown using both a theoretical metric  $\alpha$  as well as statistical evidence of reduction in metamerism on a spectral dataset comprising of 335 spectral images captured in indoor illuminations. Statistically, the third option reduces the metamerism from more than 20% to 5-8% while the first option reduces metamerism to 15-19% and the second option reduces metamerism by a very small margin only. Using two examples, one of oranges and carrots and the other of real and fake apples, we show how resolving metamers in an image can be useful for practical computer vision applications.

In conclusion, a suitably chosen fourth channel can be used for reducing metamerism of a sensor and can aid practical computer vision applications where sensor metamerism is an issue. Constrained optimization for positive valued or smooth  $\bar{F}$  may be used for a better design. In the end, we note that the currently reported results use synthesized images and the designed fourth channels have not been physically implemented. It will be interesting to consider practical implementation potentially using layered band select filters, integration of the fourth channel in a real sensor, and the associated demosaicing or multiplexing problem [30].

## Acknowledgement

This work was done during author's employment in National University of Singapore. I would like to acknowledge and thanks Dr. Michael S. Brown for the discussion on 'What can we do if we have an additional channel?'

## References

- [1] A. Alsam and R. Lenz. Calibrating color cameras using metameric blacks. *Journal of the Optical Society of America A*, 24(1):11–17, 2007. 3
- [2] R. Bala, R. Eschbach, and Y. Zhao. Substrate fluorescence: bane or boon? In *Color and Imaging Conference*, pages 12–17, 2007. 2
- [3] R. S. Berns and R. G. Kuehni. What determines crossover wavelengths of metameric pairs with three crossovers? *Color Research & Application*, 15(1):23–28, 1990. 2
- [4] M. Brown and S. Susstrunk. Multi-spectral sift for scene category recognition. In *IEEE Conference on Computer Vision and Pattern Recognition (CVPR)*, pages 177–184, 2011. 1
- [5] A. Chakrabarti and T. Zickler. Statistics of real-world hyperspectral images. In *IEEE Conference on Computer Vision and Pattern Recognition (CVPR)*, pages 193–200, 2011. 2
- [6] C. Chi, H. Yoo, and M. Ben-Ezra. Multi-spectral imaging by optimized wide band illumination. *International Journal of Computer Vision*, 86:140–151, 2010. 1
- [7] J. Cohen. Dependency of the spectral reflectance curves of the munsell color chips. *Psychonomic Science*, 1964. 2
- [8] J. B. Cohen and W. E. Kappauf. Metameric color stimuli, fundamental metamers, and wyszecki’s metameric blacks. *The American Journal of Psychology*, pages 537–564, 1982. 2, 3
- [9] M. S. Drew and R. Bala. Sensor transforms to improve metamerism-based watermarking. In *Color and Imaging Conference*, pages 22–26, 2010. 2
- [10] M. S. Drew and B. V. Funt. Natural metamers. *CVGIP: Image Understanding*, 56(2):139 – 151, 1992. 3
- [11] N. Eslahi, S. H. Amirshahi, and F. Agahian. Recovery of spectral data using weighted canonical correlation regression. *Optical Review*, 16(3):296–303, 2009. 3
- [12] H. S. Fairman and M. H. Brill. The principal components of reflectances. *Color Research & Application*, 29(2):104–110, 2004. 2
- [13] G. D. Finlayson and P. M. Morovic. Crossover wavelengths of natural metamers. *Color Image Science*, pages 10–12, 2000. 2
- [14] C. Fredembach and S. Süssstrunk. Colouring the near-infrared. In *Color and Imaging Conference*, volume 2008, pages 176–182. Society for Imaging Science and Technology, 2008. 1
- [15] C. M. Goral, K. E. Torrance, D. P. Greenberg, and B. Battaile. Modeling the interaction of light between diffuse surfaces. In *ACM SIGGRAPH Computer Graphics*, volume 18, pages 213–222, 1984. 3
- [16] J. Gu and C. Liu. Discriminative illumination: Per-pixel classification of raw materials based on optimal projections of spectral brdf. In *IEEE Conference on Computer Vision and Pattern Recognition (CVPR)*, pages 797–804, 2012. 1
- [17] P. G. Herzog, D. Knipp, H. Stiebig, and F. Koenig. Characterization of novel three- and six-channel color moire free sensors. In *Proceedings of SPIE*, volume 3648, pages 48–59, 1998. 2
- [18] C. P. Huynh and A. Robles-Kelly. A comparative evaluation of spectral reflectance representations for spectrum reconstruction, interpolation and classification. In *IEEE Conference on Computer Vision and Pattern Recognition Workshops (CVPRW)*, pages 328–335, 2013. 2
- [19] T. Jaaskelainen, J. Parkkinen, and S. Toyooka. Vector-subspace model for color representation. *Journal of the Optical Society of America A*, 7(4):725–730, 1990. 2
- [20] J. Jiang and J. Gu. Recovering spectral reflectance under commonly available lighting conditions. In *IEEE Conference on Computer Vision and Pattern Recognition Workshops (CVPRW)*, pages 1–8, 2012. 1
- [21] D. Knipp, P. Herzog, H. Stiebig, and F. König. Multi-channel sensors with reduced metameric errors. *Journal of Non-Crystalline Solids*, 266:1158–1162, 2000. 2
- [22] C. Lau, W. Heidrich, and R. Mantiuk. Cluster-based color space optimizations. In *IEEE International Conference on Computer Vision (ICCV)*, pages 1172–1179, 2011. 1
- [23] A. D. Logvinenko. Object-colour manifold. *International Journal of Computer Vision*, 101(1):143–160, 2013. 1
- [24] D. Miyazaki, K. Takahashi, M. Baba, H. Aoki, R. Furukawa, M. Aoyama, and S. Hiura. Mixing paints for generating metamerism art under 2 lights and 3 object colors. In *IEEE International Conference on Computer Vision Workshops (ICCVW)*, pages 874–882, 2013. 1
- [25] N. Ohta. Intersections of spectral curves of metameric colors. *Color Research & Application*, 12(2):85–87, 1987. 2
- [26] J. Parkkinen, J. Hallikainen, and T. Jaaskelainen. Characteristic spectra of munsell colors. *Journal of the Optical Society of America A*, 6(2):318 – 22, 1989. 2
- [27] S. Peyvandi and S. H. Amirshahi. Generalized spectral decomposition: a theory and practice to spectral reconstruction. *Journal of the Optical Society of America A*, 28(8):1545–1553, 2011. 3
- [28] D. K. Prasad. Gamut expansion of consumer camera to the cie xyz color gamut using a specifically designed fourth sensor channel. *Applied optics*, 54(20):6146–6154, 2015. 1
- [29] D. K. Prasad and L. Wenhe. Metrics and statistics of frequency of occurrence of metamerism in consumer cameras for natural scenes. *JOSA A*, 32(7):1390–1402, 2015. 6
- [30] Z. Sadeghipoor, Y. M. Lu, and S. Süssstrunk. Optimum spectral sensitivity functions for single sensor color imaging. In *IS&T/SPIE Electronic Imaging*, pages 829904–829904, 2012. 8
- [31] B. Sajadi, A. Majumder, K. Hiwada, A. Maki, and R. Raskar. Switchable primaries using shiftable layers of color filter arrays. *ACM Transactions on Graphics*, 30(4):65, 2011. 1, 2
- [32] N. Salamati, A. Germain, and S. Süssstrunk. Removing shadows from images using color and near-infrared. In *Image Processing (ICIP), 2011 18th IEEE International Conference on*, pages 1713–1716. IEEE, 2011. 1
- [33] N. Salamati and S. Süssstrunk. Material-based object segmentation using near-infrared information. In *Color and Imaging Conference*, volume 2010, pages 196–201. Society for Imaging Science and Technology, 2010. 1
- [34] D.-Y. Tzeng and R. S. Berns. Spectral-based six-color separation minimizing metamerism. In *Color and Imaging Conference*, pages 342–347, 2000. 2
- [35] G. Wyszecki. Evaluation of metameric colors. *Journal of the Optical Society of America*, 48(7):451–452, 1958. 2
- [36] F. Yasuma, T. Mitsunaga, D. Iso, and S. K. Nayar. Generalized assorted pixel camera: postcapture control of resolution, dynamic range, and spectrum. *IEEE Transactions on Image Processing*, 19(9):2241–2253, 2010. 1, 2
- [37] H. Zhao, R. Kawakami, R. T. Tan, and K. Ikeuchi. Estimating basis functions for spectral sensitivity of digital cameras. In *Meeting on Image Recognition and Understanding*, number 1, 2009. 3
- [38] Y. Zhao and R. S. Berns. Image-based spectral reflectance reconstruction using the matrix r method. *Color Research & Application*, 32(5):343–351, 2007. 3
- [39] C. Zhou and S. K. Nayar. Computational cameras: convergence of optics and processing. *IEEE Transactions on Image Processing*, 20(12):3322–3340, 2011. 1